The Protein-Tethered Lipid Bilayer: A Novel Mimic of the Biological Membrane

Frank Giess,* Marcel G. Friedrich,* Joachim Heberle,† Renate L. Naumann,* and Wolfgang Knoll*
*Max Planck Institute for Polymer Research, Mainz, Germany; and †Research Centre Juelich, Juelich, Germany

ABSTRACT A new concept of solid-supported tethered bilayer lipid membrane (tBLM) for the functional incorporation of membrane proteins is introduced. The incorporated protein itself acts as the tethering molecule resulting in a versatile system in which the protein determines the characteristics of the submembraneous space. This architecture is achieved through a metal chelating surface, to which histidine-tagged (His-tagged) membrane proteins are able to bind in a reversible manner. The tethered bilayer lipid membrane is generated by substitution of protein-bound detergent molecules with lipids using in-situ dialysis or adsorption. The system is characterized by surface plasmon resonance, quartz crystal microbalance, and electrochemical impedance spectroscopy. His-tagged cytochrome *c* oxidase (C*c*O) is used as a model protein in this study. However, the new system should be applicable to all recombinant membrane proteins bearing a terminal His-tag. In particular, combination of surface immobilization and membrane reconstitution opens new prospects for the investigation of functional membrane proteins by various surface-sensitive techniques under a defined electric field.

INTRODUCTION

Membrane proteins play a major role in every living cell. With the advances in genome mapping it was revealed that ~20–30% of the genes of an organism encode for membrane proteins (Gerstein and Hegyi, 1998). These proteins are the key factors in the cell's metabolism, for example in cell-cell interaction, signal transduction, and transport of ions and nutrients. Due to this important function, they are a preferred target for pharmaceuticals (currently >60% of consumed drugs). Additionally, membrane proteins account for the two key reactions of biochemistry: respiration and photosynthesis (Ludwig et al., 2001; Richter and Ludwig, 2003).

Contrary to this fundamental role in biology, accessibility of membrane proteins by experimental techniques remains challenging. Structural as well as functional characterization of membrane proteins is difficult due to their amphiphilic properties that interfere with crystallization necessary for x-ray crystallography. Consequently, few examples of the atomic structure of membrane proteins are reported (see Stahlberg et al., 2002; Torres et al., 2003 for review). The limitation of NMR experiments to low-molecular-weight particles forces investigators to use organic solvents or detergent solutions rather than lipid bilayer systems. Obviously all of these structural methods are unable to reflect the importance of the membrane water interface for the structural and functional properties of membrane proteins (Hurley, 2003; White et al., 2001).

Various model systems of the biological membrane address this issue. Solubilized membrane proteins are purified and reconstituted; i.e., reintegrated in an (artificial) lipid bilayer, which mimicks their native environment in the plasma membrane. In the classical liposomal system the lipid bilayer encloses an inner cavity. Therefore, experimental difficulties arise when there is a need to control contents or solute concentrations of the inner compartment. The same holds for the application of a transmembrane potential that is limited to the generation of a diffusion potential by the usage of ion-specific ionophores (Vecer et al., 1997). These problems do not arise when using black lipid membranes (BLMs) that provide equal access to both sides of a membrane. However, BLMs lack mechanical and long-term stability (Winterhalter, 2000). For both of these systems it is impossible to apply surface-sensitive techniques such as AFM, SPR, QCM, or ATR-FTIR, and will probably never evolve to a routinely used and/or large-scale technology for biosensing or lab-on-a-chip applications.

To overcome these problems, solid-supported lipid membranes were developed in the recent decade, starting from bilayers floating freely on top of a quartz, indium tin oxide, or gold surface, to polymer-supported and tethered bilayer lipid membranes (tBLMs). The latter ones address the necessity of a submembraneous space serving both as an ionic reservoir as well as providing adequate space for incorporated membrane proteins (Guidelli et al., 2001; Knoll et al., 2000; Krishna et al., 2003; Naumann et al., 2002, 2003, 1999; Raguse et al., 1998; Schiller et al., 2003; Sinner and Knoll, 2001). The most demanding problem in tBLMs is to achieve electrical properties that are competitive with BLMs, i.e., show a capacitance of ~0.5 μF/cm^2 and resistances >1 MΩ cm^2 (Krishna et al., 2001; Naumann et al., 2003; Peggion et al., 2001; Schiller et al., 2003). Albeit many different systems were developed in the recent years, few show the functional incorporation of complex membrane proteins (Naumann et al., 2002, 1999; Schmidt et al., 1998; Sevin-Landais et al., 2000) .

Submitted May 21, 2004, and accepted for publication July 7, 2004.

Address reprint requests to Renate L. Naumann, E-mail: naumannr@mpip-mainz.mpg.de.

0006-3495/04/11/3213/08 $2.00

doi: 10.1529/biophysj.104.046169

All tBLMs reported to date are defined by bifunctional molecules, providing a lipophilic domain and a hydrophilic spacer. The lipophilic part inserts into one or both leaflets of the lipid membrane and can consist of phospholipids (Naumann et al., 2002, 1999; Peggion et al., 2001; Schmidt et al., 1998), cholesterols (Becucci et al., 2002; Lang et al., 1994), alkyl chains (Cornell et al., 1997; Glazier et al., 2000; Williams et al., 1997) or phytanyl groups (Cornell et al., 2001; Krishna et al., 2001; Naumann et al., 2003; Raguse et al., 1998; Schiller et al., 2003; Terrettaz et al., 2003; Vanderah et al., 1998; Woodhouse et al., 1998). The hydrophilic spacer attaches the tethering molecule to the support and determines the hydrophilic environment as well as the volume of the submembraneous space. Successful applications of polyethylene oxide (Naumann et al., 2003; Schiller et al., 2003; Terrettaz et al., 2003) and peptide spacer groups were reported for the generation of highly insulating tBLM systems (Peggion et al., 2001), necessary to investigate membrane proteins under a defined electric field.

However, the tethering molecules inevitably apply diffusional constraints to the lipid molecules of the tBLM in a way as to prevent the membrane protein to undergo conformational or diffusional changes necessary for its biological activity. Furthermore the tethering portion may not be compatible with bulky extramembraneous domains. Finally, the tethering part requires a certain amount of space that is not accessible to the protein, water, or ions.

To overcome these limitations, a tBLM was developed with the membrane protein of interest being the essential building block. The necessary surface modification is based on the concept of the well-established metal ion affinity chromatography (Hochuli et al., 1987). Ion chelating nitrilotriacetic acid groups bearing a terminal amino group (ANTA) are coupled in situ to an *N*-hydroxy succinimide (NHS) ester functionalized surface. The resulting NTA surface is activated by complexation of Cu^{2+} ions rendering it capable of reversible immobilization of His-tagged proteins (see Fig. 1).

The generation of a protein-tethered bilayer lipid membrane (ptBLM) on top of the NTA surface is illustrated schematically in Fig. 2. The His-tagged membrane protein is first attached to the surface in its detergent solubilized form. In the second step, the detergent molecules are substituted by lipid molecules thus forming a lipid bilayer that is tethered to the support by the protein itself. The coupling His-tag provides sufficient intramolecular flexibility to allow for activity in the reconstituted protein. Above all, it renders the proposed method universally applicable to all His-tagged membrane proteins.

Both, in situ affinity coupling of proteins (Kroger et al., 1999; Madoz-Gurpide et al., 2000; Rigler et al., 2003) and in-situ dialysis (Devadoss and Burgess, 2002; Singh and Keller, 1991) were described before. However, the idea to combine the two to form a membrane protein-tethered lipid bilayer is new. First examples of the experimental power of the new system are demonstrated by the use of surface analytical methods such as surface plasmon resonance (SPR) and by quartz crystal microbalance (QCM) measurements. In particular, electrochemical impedance spectroscopy (EIS) is used, with C*c*O from *Rhodobacter sphaeroides* as a model protein, to measure active proton transport catalyzed by dioxygen reduction (Wikstrom, 2004).

MATERIALS

If not otherwise stated all chemicals including equine heart cyt *c* were purchased from Sigma-Aldrich Chemie GmbH (Munich, Germany). 1,2-diphytanoyl-*sn*-glycero-3-phosphocholine (DiPhyPC) was obtained from Avanti Polar Lipids (Alabaster, AL). C*c*O from *R. sphaeroides* with the

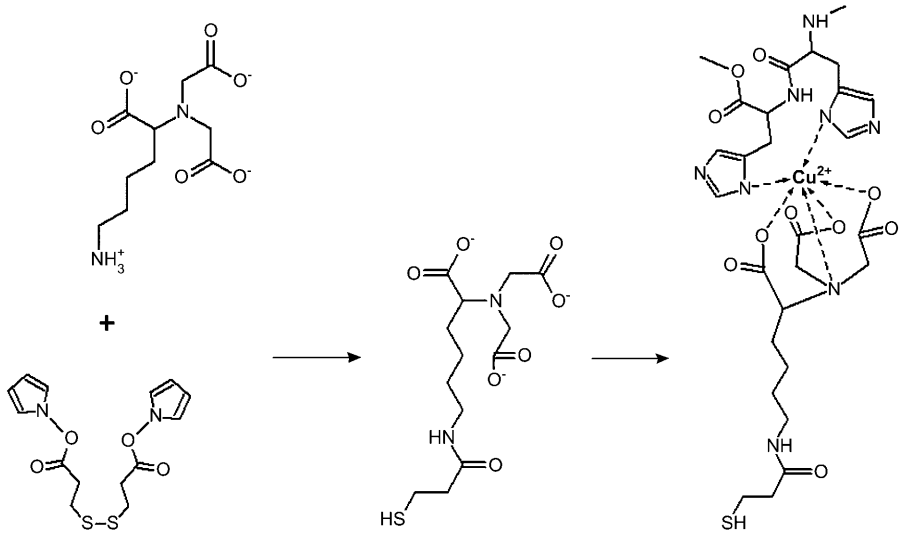

FIGURE 1 Coupling reaction leading to the chelating surface. An NHS-activated monolayer is prepared by self-assembly of DTSP (*left*) that is thereafter coupled with ANTA (*middle*). Complex formation is achieved by immersing the electrode in $CuSO_4$ solution, ready for complexation with the His-tagged C*c*O (*right*).

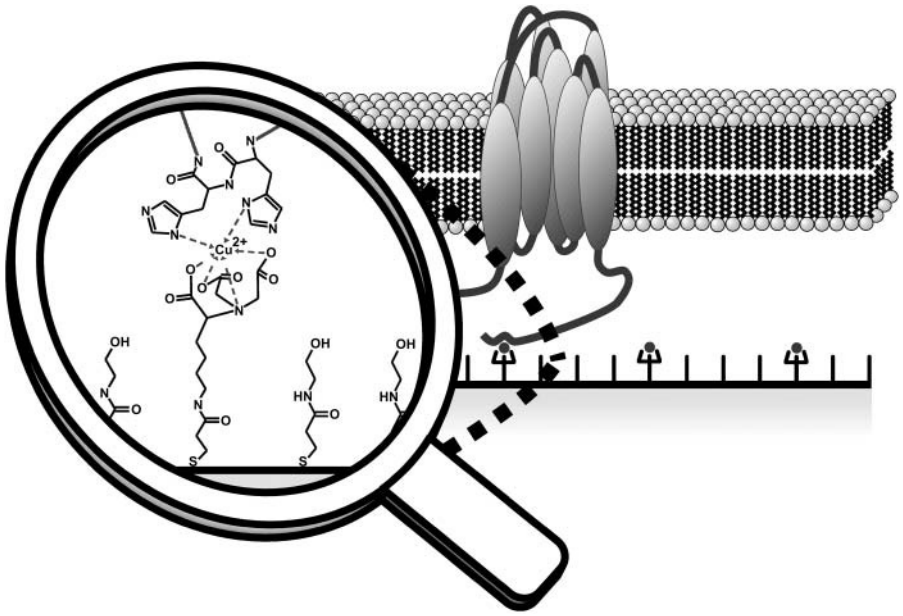

FIGURE 2 Conceptual representation of the protein-tethered lipid bilayer. The interaction between the terminal His-tag of the membrane protein and the NTA functionality is magnified at the left side. Note that the size of the His-tagged hydrophilic domain will determine the submembraneous space. The figure is not drawn to scale.

His-tag fused to the C-terminus of subunit I was expressed and purified according to Mitchell and Gennis (1995).

The protein was solubilized in PBS/DDM buffer (100 mM KCl, 50 mM phosphate, pH 8 0.1% dodecyl maltoside (DDM)). Buffer and detergent concentrations were kept constant during the binding experiments. To probe the reversibility of the binding, PBS/DDM buffer was substituted with a buffer of the same composition, albeit with additional 100 mM imidazole. For dialysis pure PBS buffer (without detergent) was used.

METHODS

Preparation of the template stripped gold (TSG) electrodes was done as described (Naumann et al., 2003): briefly, 50-nm-thick gold films were deposited by electrothermal evaporation (rate 0.01–0.05 nm/s, 2 10^{-6} mbar) on silicon wafers (roughness according to AFM was <1 nm). Gold films on silicon wafers were then glued with EPO-TEK 353ND-4, ($n = 1.5922$) to LaSFN9 high index match glass slides and cured for 60 min at 150°C. The silicon wafer was detached from the gold film just before use.

Quartz crystals (Q-Sense AB, Vaestra Froelunda, Sweden) were cleaned in an H_2O_2-NH_3-water solution (1:1:5, 70°C for 10 min) and rinsed with water and ethanol.

Functionalization of the gold films

Both glass slides and cleaned quartz crystals, to be prepared for SPR/EIS and QCM measurements, respectively, were immersed for 30 min in a solution of dithiobis (*N*-succinimidyl propionate) (DTSP; see Fig. 2) in dry DMSO (2 mg/ml). The slides were rinsed with dry DMSO, water, and ethanol and dried in a stream of nitrogen. The slides were then immersed for 2 h in a 0.15-M solution of *N*-(5-amino-1-carboxypentyl) iminodiacetic acid (ANTA) buffered to pH 9.8 by adding 0.5 M KCO_3. As a last step the glass slide was immersed for 30 min in 40 mM $CuSO_4$ in acetate buffer (50 mM, pH 5.5). After Cu^{2+} incubation the slides were rinsed with water and PBS buffer.

Reversible protein binding and lipid reconstitution by in-situ dialysis

The protein solution was infused into the SPR or the QCM cell, respectively, by pumping 500 μl aliquots of an 830-nM protein solution at a constant velocity of 250 μl/min, followed by immediate washing with PBS/DDM buffer. Subsequently, the solution was exchanged to the imidazole-containing PBS/DDM buffer and thereafter back to the imidazole-free PBS/DDM solution, completing one cycle of protein binding/desorption.

For the reconstitution, the bound protein was incubated with buffer containing solubilized DiPhyPC at a concentration 0.05 mg/ml in PBS/DDM. After 45 min the detergent was removed by pumping pure PBS buffer through the outer compartment of the dialysis cell. As an alternative to dialysis, the detergent was removed by adding biobeads to the PBS/DDM buffer (Bio-Rad Laboratories GmbH, Munich, Germany).

Surface plasmon resonance measurements

Surface plasmon resonance measurements were performed in a homebuilt SPR setup allowing for simultaneous EIS measurements as described before (Naumann et al., 1999). Surface plasmons were excited by a He/Ne laser ($\lambda = 632.8$ nm). SPR spectra were simulated using a four-layer model representing the prism glass, gold, DTSP-ANTA/protein, and lipid with refractive indices of $n = 1.7$, 3.1, 1.45, 1.5, respectively. The refractive index of the PBS buffer was assumed at $n = 1.33$. Measurements were carried out in a custom-made sandwiched dialysis cell, made from Plexiglas (see Fig. 3), separated by a dialysis membrane (molecular weight cutoff of 6000) generating an inner sample compartment ($\sim$150 μl) and an outer compartment. Dialysis was achieved by circulation of pure buffer through the outer compartment.

Electrochemical impedance spectroscopy measurements

Electrochemical impedance spectroscopy measurements were conducted using an EG&G potentiostat (model 273A, Princeton Applied Research Group, Oak Ridge, TN), controlled by a FRA analyzer (model 1260, Solartron Analytical, Farnborough, UK). Spectra were recorded over

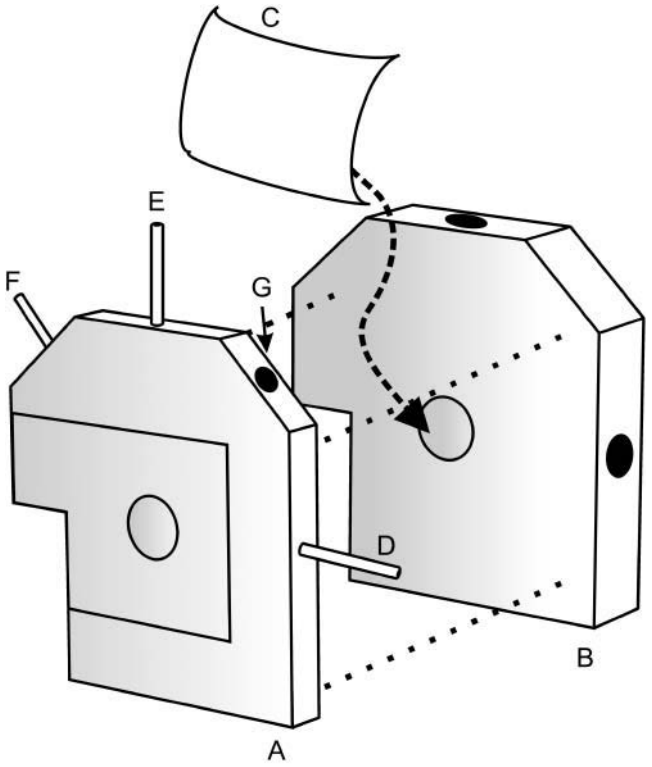

FIGURE 3 Basic cell design used for simultaneous measurements of SPR and EIS. A dialysis membrane (*C*) is placed between the two parts. The gold electrode is pressed to the front part (*A*) thus defining the sample compartment. For dialysis buffer solution is pumped continuously through the rear compartment (*B*). Proper sealing is achieved by O-rings. Sample inlet (*D*), sample outlet (*E*), connection to counter electrode (*F*), bore hole for reference electrode (*G*).

a frequency range of 3 mHz to 1 MHz with an excitation amplitude of 10 mV and a bias potential of 0 V against a $Ag/AgCl/KCl_{sat}$ reference electrode (with a platinum wire as counter electrode). Spectra were recorded firstly after immobilization of C*c*O, then after reconstitution and at last after activation. Data were subsequently analyzed by the complex nonlinear fitting algorithm supplied in ZVIEW (Version 2.6, Scribner Associates, Southern Pines, NC).

Cytochrome *c* (cyt *c*) from equine heart was used as the electron donor for C*c*O. The reduced form of cyt *c* was obtained by reaction with sodium dithionite. The excess reducing agent was removed by gel filtration through a Sephadex column. Activation was triggered by adding 20 μl of reduced cyt *c* solution (4 mg/ml), giving a final concentration of 40 mM.

Quartz crystal microbalance measurements

All quartz crystal microbalance (QCM) measurements were performed on a QSense D300 multifrequency QCM (Q-Sense AB, Vaestra Froelunda, Sweden) in a flow-through cell. Data from 5 MHz, 15 MHz, 25 MHz, and 35 MHz were collected. Reconstitution was achieved by gradually lowering the detergent concentration. The 5-MHz AC cut quartz crystals had an active surface area of $\sim$0.2 cm^2.

RESULTS AND DISCUSSION

SPR monitoring of the C*c*O binding process

The thickness of the individual dielectric layers on the gold film is determined by surface plasmon resonance spectroscopy (SPS). Reflectivity scans versus the angle of incident light are recorded (not shown). The simulation of these scans in terms of the four-layer model (see Methods) yields the thickness of the different layers listed in Table 1. SPS recordings, however, indicate the optical thickness of the dielectric layer as well as the refractive index of the bathing solution. Hence the reflectivity as a function of time at a fixed angle of incidence shown in Figs. 4 and 5 contains information not only about the thickness of the layers but also about changes in the refractive index of the buffer solution.

The thickness of the DTSP-SAM as well as the thickness change due to the coupling of ANTA are both too small to be accurately determined by SPR (see Table 1) considering that the coupling reaction consists of the substitution of the NHS residue with the ANTA molecule. The estimated length of the entire construct is $\sim$1 nm. However, the formation of these layers can be clearly detected by surface-enhanced infrared absorption spectroscopy (SEIRAS) (Ataka and Heberle, 2003) as will be shown in a forthcoming article. Changing pure PBS buffer against DDM containing buffer results in a shift of the angle of total reflection as well as an increase in reflectivity. This was simulated by a change in the bulk refractive index and additionally by a layer thickness increase of 0.9 nm. The thickness increase indicates an accumulation of detergent molecules at the surface also found by QCM measurements described below. A further increase of reflectivity is observed if C*c*O binds to the surface as shown in the kinetic trace of the SPR signal (Fig. 4, point *A*). Extensive washing with buffer results in a minor loss of material. Addition of the imidazole-containing buffer (Fig. 4, point *B*) results in a further increase in reflectivity that is attributed to a mere change of the refractive index of the bulk solution. The reflectivity returns to almost the same level as the one before protein adsorption if the imidazole buffer is replaced by the original PBS/DDM buffer (Fig. 4, point *C*). This indicates an almost complete desorption of C*c*O is from the surface as imidazole molecules compete with the His-tag for the binding sites at the Cu^{2+}/NTA complex. Nonetheless a second addition of another aliquot of C*c*O (Fig. 4, point *D*) leads to similar increase in reflectivity as the first one, showing that the adsorption of C*c*O is reversible and mediated by the interaction of the His-tag with the Cu^{2+}/NTA complex. Table 1 lists the thickness increment at each functionalization step.

Functional incorporation of C*c*O requires the enzyme to remain in its native conformation. The metal affinity surface

TABLE 1 Thickness increments linked to the different preparation stages: SPR versus QCM

Adsorption step	Δd_{SPR}/nm	Δd_{QCM}/nm*
DTSP-ANTA	0.3 ± 0.2	N/D
Cu^{2+}	0.3 ± 0.2	N/D
DDM	0.9 ± 0.2	2.6 ± 0.3
C*c*O	2.1 ± 0.3	5.5 ± 0.3

*Fitted according to the Voigt model.

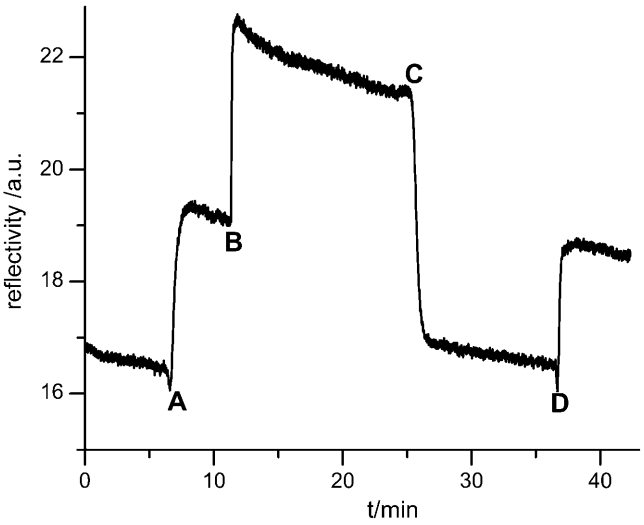

FIGURE 4 Reversible binding of C*c*O monitored by SPR. The cell is first filled with DDM/PBS. Into this solution, solubilized C*c*O is infused at points *A* and *D*, respectively, indicating the thickness increase due to binding of C*c*O. At point *B* the cell is rinsed with DDM/PBS containing 200 mM imidazole. The strong increase is due to change of refractive index. At point *C* the cell is flooded again with pure DDM/PBS changing the refractive index back to the initial value. The resulting reflectivity shows that almost complete desorption is achieved. When a new portion of solubilized C*c*O is infused at point *D* the increase in reflectivity indicates binding to be fully reversible.

causes two distinct effects both of which should promote the formation of ptBLMs: binding of the protein by the His-tag moiety prearranges the protein to form a uniform array of molecules with the His-tag in close proximity to the surface. Thus the orientation of the protein with respect to the membrane normal is dependent on the location of the histidine stretch within the protein. Consequentially, it should be possible to selectively define a vectorial ptBLM by alternation of the His-tag position. Another effect is the promotion of high surface concentrations of protein. Although not necessarily demanding for highly insulating ptBLMs, this is a key advantage of ptBLMs with respect to ''classical'' tBLM. Accumulation of the protein at the surface can be controlled by the surface concentration of the binding molecules. The lipid molecules then fill in the gaps during the last step of the reconstitution.

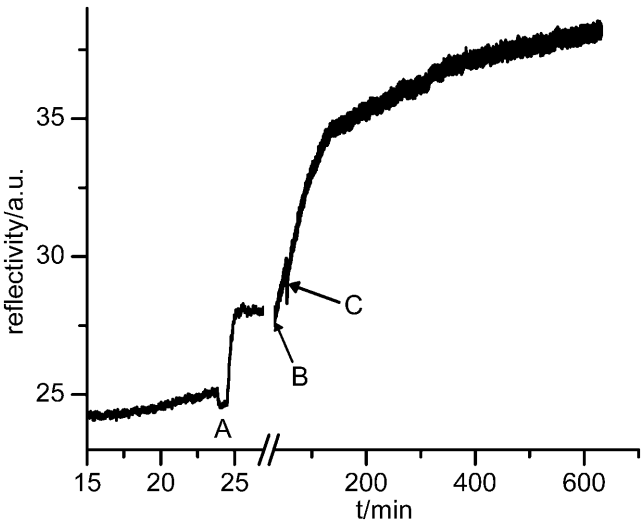

FIGURE 5 Binding of C*c*O and reconstitution monitored by SPR. At point *A*, C*c*O is infused in a DDM/PBS solution. The increase in reflectivity indicates adsorption. At point *B*, the cell is incubated with the lipid/DDM/PBS solution and dialysis sets in at point *C*. Note the different timescales.

Reconstitution of C*c*O in the bound state

The generation of a ptBLM is completed by replacing detergent molecules of the bound protein by lipids, thus forming small patches of lipid bilayers between the protein molecules, which eventually would seal the whole assembly to a closed membrane.

The design of our SPR dialysis cell allows monitoring the reconstitution process in real time. As shown in Fig. 5, the increase in reflectivity at point *A* indicates protein binding because a change in the refractive index is not involved (composition of the solution is unchanged). At point *B* the lipid/DDM/buffer is infused resulting in a change in refractive index, whereas point *C* indicates the onset of dialysis (note the different timescales). Simultaneously with the increase in reflectivity during dialysis, the electrical capacitance of the layer decreases and the resistance increases (see also Fig. 6), as described below. The combined findings are explained in terms of the successful incorporation of lipid molecules. However, the absolute thickness increment due to incorporation of lipid as estimated by SPS is not given in Table 1, because the exact degree of substitution of detergent molecules by lipid molecules is hard to assess.

QCM measurements

The resonant frequency of the quartz crystal depends on the total oscillating mass. When a thin film is adsorbed to the crystal the frequency decreases. If the film is rigid the decrease in frequency is proportional to the mass of the film. The mass of the adhering layer is calculated by using the Sauerbrey relation (Sauerbrey, 1959):

$$\Delta f = -\Delta m/nC,$$

where C is the mass sensitivity constant ($C = 17.7$ ng·cm^{-2}·Hz^{-1} at 5 MHz) and n is the overtone number ($n = 1, 3, \ldots$).

A ''soft'' (viscolelastic) film (e.g., lipids, proteins, or coupled water) will not fully couple to the oscillation of the crystal leading to a damping of the oscillation. In this case the Sauerbrey relation is not valid anymore. The dissipation of the oscillation energy contains information about the viscoelastic properties of the film.

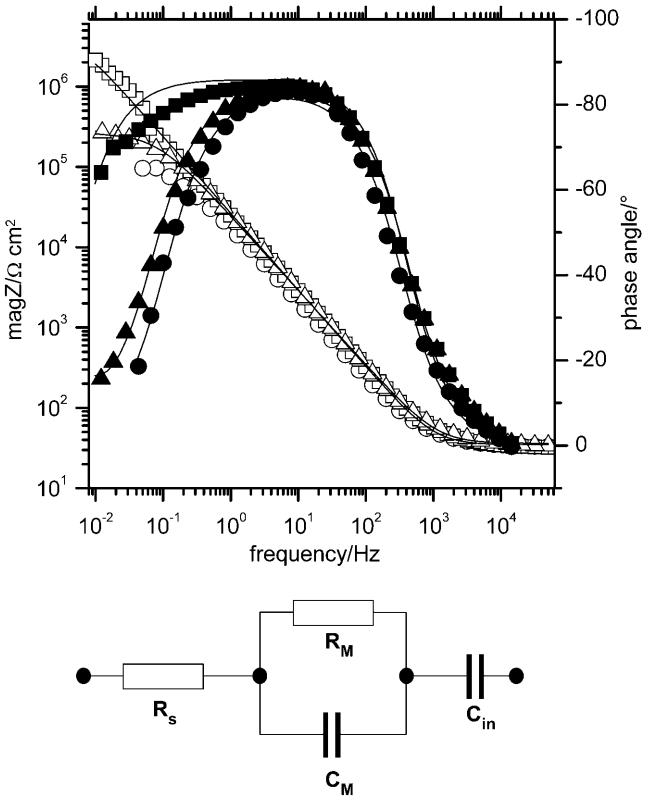

FIGURE 6 Impedance spectra measured at different stages of the experiment. Adsorbed C*c*O (Δ, ▲); after dialysis for 12 h (□, ■); after activation with cyt *c* (○, ●). Equivalent circuit used to fit the electrochemical data are: R_s solution resistance; R_m resistance of the lipid membrane; and C_m capacitance of the lipid membrane.

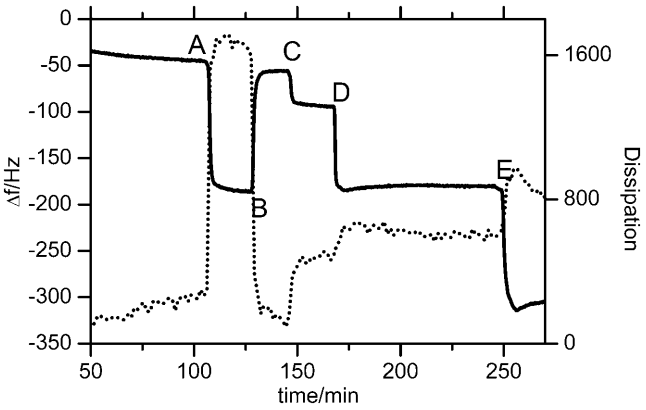

FIGURE 7 Frequency shift (*solid line*) and dissipation (*dotted line*) at different stages of the binding experiment, measured by QCM. The DTSP-NTA SAM was prepared ex situ. At point *A* the cell was flushed with 40 mM $CuSO_4$ buffer that is changed to pure water at point *B*. Points *C* and *D* indicate perfusion with PBS and PBS/DDM, respectively. C*c*O was added at point *E*.

Incubation of the NTA surface with Cu^{2+} ions results in a slight decrease in frequency shift, whereas the dissipation remains constant (see Fig. 7). According to the Sauerbrey model this frequency shift corresponds to a mass adsorption of 42 ng/cm^2, or in other terms to an area of 16.5 Å^2 for each bound Cu^{2+} ion (disregarding any contribution from surface roughness). This value fits well to the cross-sectional area of a modeled DTSP-ANTA molecule (~17 Å^2). Because the NTA/Cu^{2+} complex has a high formation constant (Arnold, 1992), all NTA residues are complexed by Cu^{2+}. Therefore, DTSP should form a closely packed layer on the gold film that reacts quantitatively with ANTA.

Adsorption of DDM and C*c*O at the surface results in a decreasing resonance frequency as well as in an increasing dissipation. Hence the adsorbed mass was determined by fitting according to a Voigt-based viscoelastic model. Considerable differences between thickness values determined by SPR and the QCM measurements are observed (Table 1). QCM is not only sensitive to the directly adsorbed mass, but also to entrapped and closely coupled molecules, e.g., water. Although this surface coupled water does not contribute to an increase in optical thickness and hence is invisible in SPR, it adds a notable amount of viscoelastic mass, which is detected by the QCM. The reconstitution could not be measured by the QCM because of the design of the flow cell that did not allow for an in-situ dialysis.

EIS measurements

EIS spectra were recorded after every preparation step described above. Capacitance and resistance values obtained by fitting the data to the equivalent circuit shown in the insert of Fig. 6 are given in Table 2.

The resistance of the NTA-DTSP SAM decreases somewhat upon complexation of Cu^{2+} ions (not shown). A similar effect has been reported by Madoz-Gurpide et al. (2000) and was attributed to the shielding of the negative surface charges by complexed Cu^{2+} ions.

Incubation of the complexed monolayer with DDM containing buffer as well as the binding of C*c*O to the surface did not lead to significant changes in resistance and capacitance. Further incubation with lipid containing buffer and, in particular, the removal of detergent by dialysis, however, increased the resistance to values higher than 800 kΩ·cm^2 whereas the capacitance decreased considerably to

TABLE 2 Resistance and capacitance values from EIS data fitted to the equivalent circuit given in Fig. 6 for different preparation steps

	Resistance/kΩ·cm^2	Capacitance/μF/cm^2
DTSP-ANTA-Cu^{2+}-C*c*O complex	35 ± 10	10 ± 2
Reconstituted	800 ± 300	6 ± 1
After activation	100 ± 20	6 ± 1
After washing	750 ± 300	6 ± 1
After activation in the presence of KCN	750 ± 300	7 ± 1

$\sim$6 μF cm^{-2}. Examples of EIS spectra are shown in Fig. 6. This finding is consistent with the formation of a lipid bilayer, although the numerical values obtained are not those expected for a perfect bilayer lipid membrane, which should have capacitances approaching 0.5 μF cm^{-2} and resistances $>$1 MΩ cm^2. It has to be considered, however, that ptBLMs contain a large amount of protein with a dielectric constant higher than that of the lipid. From this the capacitance of the system is expected to be higher than that of the pure lipid bilayer. Assuming a dielectric constant of 30 for C*c*O (Smith et al., 1993) and 2 for DiPhyPC, the overall capacitance is estimated to be in the range of 2 μF cm^{-2} for a bilayer thickness of 5 nm and a protein content of 30%. To test whether or not the reconstituted C*c*O can be activated under these conditions, reduced cyt *c* was added to the oxygenated solution to obtain a final concentration of 40 mM. The impedance spectrum showed a drastic decrease in resistance (see the example shown in Fig. 6 from $>$1 MΩ cm^2) to 130 kΩ cm^2 indicating that the protein actively transports protons during the catalytic redox cycle. After washing off the cyt *c* with PBS, the resistance returned to the previous value illustrating that the activation is fully reversible. Infusion of reduced cyt *c* together with 0.6 mM KCN, on the other hand, did not lead to a decrease in resistance, showing that in this case the C*c*O is specifically inhibited. Electrical data are collected in Table 2 for comparison.

CONCLUSION

Protein-tethered bilayer lipid membranes have been shown to be a feasible concept to reconstitute complex membrane proteins in a tethered lipid bilayer system. Because affinity metal chromatography is a routinely applied protein purification system, ptBLMs can be seen as a universally applicable system for immobilization and surface-focused reconstitution of His-tagged membrane proteins. Purification of the proteins could even be avoided, if the preparation of ptBLMs would be performed using the crude cell lysate. This allows for the application of integrated proteomics (for review see Catimel et al., 2001) to membrane proteins.

EIS spectra before and after the addition of reduced cyt *c* show unequivocally that the enzyme is in the active state and that the activation is fully reversible. This opens new possibilities to investigate enzyme-catalyzed ion transport as a function of a defined transmembrane potential. The respective investigation in the case of the C*c*O is currently under way.

Preliminary studies have shown that activation can be followed by electrochemical and spectroscopic techniques simultaneously. Using roughened silver or gold films as the substrate for the ptBLM surface-enhancement techniques like SERRS (surface enhanced resonance Raman spectroscopy) (Wackerbarth et al., 1999) and SEIRAS (Heberle and Ataka, 2004) can be applied as will be shown in forthcoming articles. Surface analytical techniques can be exploited, like SPR and QCM as shown above, as well as AFM and STM. The immobilization procedure provides the advantage that the surface concentration of the protein can be optimized individually for every single technique.

As far as ion transport is concerned but also for structural studies, a critical issue for all membrane systems tethered to surfaces is the submembrane space. The advantage of the ptBLM is that the cytosolic part of the protein itself defines the submembrane space. In the case of the C*c*O this seems to be sufficiently large to allow for ion transport to occur across the lipid bilayer as demonstrated by EIS. Nonetheless, it is also possible to design longer affinity spacer molecules to expand the submembraneous space thus changing the electrochemical properties of the system. This is facilitated by the simplicity of the developed surface chemistry that is based exclusively on commercially available chemicals. Preliminary experiments using two coupling steps to engraft an oligoethylene glycol moiety between the Au anchor and the affinity tag showed already-promising results.

In summary, the ptBLM seems to open up promising new ways to investigate membrane proteins in a biomimetic lipid environment.

REFERENCES

Arnold, F. H. 1992. Metal Affinity Protein Separations. Academic Press, San Diego, CA.

Ataka, K., and J. Heberle. 2003. Electrochemically induced surface-enhanced infrared difference absorption (SEIDA) spectroscopy of a protein monolayer. *J. Am. Chem. Soc.* 125:4986–4987.

Becucci, L., R. Guidelli, Q. Y. Liu, R. J. Bushby, and S. D. Evans. 2002. A biomimetic membrane consisting of a polyethyleneoxythiol monolayer anchored to mercury with a phospholipid bilayer on top. *J. Phys. Chem. B.* 106:10410–10416.

Catimel, B., J. Rothacker, and E. Nice. 2001. The use of biosensors for microaffinity purification: an integrated approach to proteomics. *J. Biochem. Biophys. Methods.* 49:289–312 [Review].

Cornell, B. A., V. L. B. Braachmaksvytis, L. G. King, P. D. J. Osman, B. Raguse, L. Wieczorek, and R. J. Pace. 1997. A biosensor that uses ion-channel switches. *Nature.* 387:580–583.

Cornell, B. A., G. Krishna, P. D. Osman, R. D. Pace, and L. Wieczorek. 2001. Tethered-bilayer lipid membranes as a support for membrane-active peptides. *Biochem. Soc. Trans.* 29:613–617.

Devadoss, A., and J. D. Burgess. 2002. Detection of cholesterol through electron transfer to cholesterol oxidase in electrode-supported lipid bilayer membranes. *Langmuir.* 18:9617–9621.

Gerstein, M., and H. Hegyi. 1998. Comparing genomes in terms of protein structure: surveys of a finite parts list. *FEMS Microbiol. Rev.* 22:277–304.

Glazier, S. A., D. J. Vanderah, A. L. Plant, H. Bayley, G. Valincius, and J. J. Kasianowicz. 2000. Reconstitution of the pore-forming toxin alpha-hemolysin in phospholipid/18-octadecyl-1-thiahexa(ethylene oxide) and phospholipid/n-octadecanethiol supported bilayer membranes. *Langmuir.* 16:10428–10435.

Guidelli, R., G. Aloisi, L. Becucci, A. Dolfi, M. R. Moncelli, and F. T. Buoninsegni. 2001. New directions and challenges in electrochemistry: bioelectrochemistry at metal/water interfaces. *J. Electroanal. Chem.* 504:1–28 [Review].

Heberle, J., and K. Ataka. 2004. SEIDAS: oberflächenverstärkte differenzspektroskopie zur funktionellen untersuchung von proteinmonolagen. *Biospektrum.* 10:42–44. [in German].

Hochuli, E., H. Dobeli, and A. Schacher. 1987. New metal chelate adsorbent selective for proteins and peptides containing neighbouring histidine residues. *J. Chromatogr.* 411:177–184.

Hurley, J. H. 2003. Membrane proteins: adapting to life at the interface. *Chem. Biol.* 10:2–3.

Knoll, W., C. W. Frank, C. Heibel, R. Naumann, A. Offenhausser, J. Ruhe, E. K. Schmidt, W. W. Shen, and A. Sinner. 2000. Functional tethered lipid bilayers. *J. Biotechnol.* 74:137–158.

Krishna, G., J. Schulte, B. A. Cornell, R. J. Pace, and P. D. Osman. 2003. Tethered bilayer membranes containing ionic reservoirs: selectivity and conductance. *Langmuir.* 19:2294–2305.

Krishna, G., J. Schulte, B. A. Cornell, R. Pace, L. Wieczorek, and P. D. Osman. 2001. Tethered bilayer membranes containing ionic reservoirs: the interfacial capacitance. *Langmuir.* 17:4858–4866.

Kroger, D., M. Liley, W. Schiweck, A. Skerra, and H. Vogel. 1999. Immobilization of histidine-tagged proteins on gold surfaces using chelator thioalkanes. *Biosens. Bioelectron.* 14:155–161.

Lang, H., C. Duschl, and H. Vogel. 1994. A new class of thiolipids for the attachment of lipid bilayers on gold surfaces. *Langmuir.* 10:197–210.

Ludwig, B., E. Bender, S. Arnold, M. Huttemann, I. Lee, and B. Kadenbach. 2001. Cytochrome c oxidase and the regulation of oxidative phosphorylation. *Chembiochem.* 2:392–403.

Madoz-Gurpide, J., J. M. Abad, J. Fernandez-Recio, M. Velez, L. Vazquez, C. Gomez-Moreno, and V. M. Fernandez. 2000. Modulation of electroenzymatic NADPH oxidation through oriented immobilization of ferredoxin: NADP(+) reductase onto modified gold electrodes. *J. Am. Chem. Soc.* 122:9808–9817.

Mitchell, D. M., and R. B. Gennis. 1995. Rapid purification of wildtype and mutant cytochrome c oxidase from Rhodobacter sphaeroides by Ni2+-Nta affinity chromatography. *FEBS Lett.* 368:148–150.

Naumann, R., T. Baumgart, P. Graber, A. Jonczyk, A. Offenhausser, and W. Knoll. 2002. Proton transport through a peptide-tethered bilayer lipid membrane by the H^+-ATP synthase from chloroplasts measured by impedance spectroscopy. *Biosens. Bioelectron.* 17:25–34.

Naumann, R., S. M. Schiller, F. Giess, B. Grohe, K. B. Hartman, I. Karcher, I. Koper, J. Lubben, K. Vasilev, and W. Knoll. 2003. Tethered lipid bilayers on ultraflat gold surfaces. *Langmuir.* 19:5435–5443.

Naumann, R., E. K. Schmidt, A. Jonczyk, K. Fendler, B. Kadenbach, T. Liebermann, A. Offenhausser, and W. Knoll. 1999. The peptide-tethered lipid membrane as a biomimetic system to incorporate cytochrome c oxidase in a functionally active form. *Biosens. Bioelectron.* 14:651–662.

Peggion, C., F. Formaggio, C. Toniolo, L. Becucci, M. R. Moncelli, and R. Guidelli. 2001. A peptide-tethered lipid bilayer on mercury as a biomimetic system. *Langmuir.* 17:6585–6592.

Raguse, B., V. Braachmaksvytis, B. A. Cornell, L. G. King, P. D. J. Osman, R. J. Pace, and L. Wieczorek. 1998. Tethered lipid bilayer membranes: formation and ionic reservoir characterization. *Langmuir.* 14:648–659.

Richter, O. M., and B. Ludwig. 2003. Cytochrome c oxidase: structure, function, and physiology of a redox-driven molecular machine. *Rev. Physiol. Biochem. Pharmacol.* 147:47–74.

Rigler, P., W. P. Ulrich, P. Hoffmann, M. Mayer, and H. Vogel. 2003. Reversible immobilization of peptides: surface modification and in situ detection by attenuated total reflection FTIR spectroscopy. *Chemphyschem.* 4:268–275.

Sauerbrey, G. 1959. Verwendung von Schwingquarzen zur Wägung dünner Schichten und zur Mikrowägung. *Z. Phys.* 155:206–222. (In German).

Schiller, S. M., R. Naumann, K. Lovejoy, H. Kunz, and W. Knoll. 2003. Archaea analogue thiolipids for tethered bilayer lipid membranes on ultrasmooth gold surfaces. *Angewandte Chemie-International Edition.* 42:208–210.

Schmidt, E. K., T. Liebermann, M. Kreiter, A. Jonczyk, R. Naumann, A. Offenhausser, E. Neumann, A. Kukol, A. Maelicke, and W. Knoll. 1998. Incorporation of the acetylcholine receptor dimer from Torpedo californica in a peptide supported lipid membrane investigated by surface plasmon and fluorescence spectroscopy. *Biosens. Bioelectron.* 13:585–591.

Sevin-Landais, A., P. Rigler, S. Tzartos, F. Hucho, R. Hovius, and H. Vogel. 2000. Functional immobilisation of the nicotinic acetylcholine receptor in tethered lipid membranes. *Biophys. Chem.* 85:141–152.

Singh, S., and D. Keller. 1991. Atomic force microscopy of supported planar membrane bilayers. *Biophys. J.* 60:1401–1410.

Sinner, E. K., and W. Knoll. 2001. Functional tethered membranes. *Curr. Opin. Chem. Biol.* 5:705–711.

Smith, P. E., R. M. Brunne, A. E. Mark, and W. F. Van Gunsteren. 1993. Dielectric properties of trypsin inhibitor and lysozyme calculated from molecular dynamics simulations. *J. Phys. Chem.* 97:2009–2014.

Stahlberg, H., A. Engel, and A. Philippsen. 2002. Assessing the structure of membrane proteins: combining different methods gives the full picture. *Biochem. Cell Biol.* 80:563–568.

Terrettaz, S., M. Mayer, and H. Vogel. 2003. Highly electrically insulating tethered lipid bilayers for probing the function of ion channel proteins. *Langmuir.* 19:5567–5569.

Torres, J., T. J. Stevens, and M. Samso. 2003. Membrane proteins: the ''Wild West'' of structural biology. *Trends Biochem. Sci.* 28:137–144.

Vanderah, D. J., C. W. Meuse, V. Silin, and A. L. Plant. 1998. Synthesis and characterization of self-assembled monolayers of alkylated 1-thiahexa(ethylene oxide) compounds on gold. *Langmuir.* 14:6916–6923.

Vecer, J., P. Herman, and A. Holoubek. 1997. Diffusion membrane potential in liposomes: setting by ion gradients, absolute calibration and monitoring of fast changes by spectral shifts of Dis-C-3(3) fluorescence maximum. *Biochim. Biophys. Acta.* 1325:155–164.

Wackerbarth, H., U. Klar, W. Gunther, and P. Hildebrandt. 1999. Novel time-resolved surface-enhanced (resonance) Raman spectroscopic technique for studying the dynamics of interfacial processes: application to the electron transfer reaction of cytochrome c at a silver electrode. *Appl. Spectrosc.* 53:283–291.

White, S. H., A. S. Ladokhin, S. Jayasinghe, and K. Hristova. 2001. How membranes shape protein structure. *J. Biol. Chem.* 276:32395–32398.

Wikstrom, M. 2004. Cytochrome c oxidase: 25 years of the elusive proton pump. *Biochim. Biophys. Acta.* 1655:241–247.

Williams, L. M., S. D. Evans, T. M. Flynn, A. Marsh, P. F. Knowles, R. J. Bushby, and N. Boden. 1997. Kinetics of the unrolling of small unilamellar phospholipid vesicles onto self-assembled monolayers. *Langmuir.* 13:751–757.

Winterhalter, M. 2000. Black lipid membranes. *Curr. Opin. Colloid Interface Sci.* 5:250–255 [Review].

Woodhouse, G. E., L. G. King, L. Wieczorek, and B. A. Cornell. 1998. Kinetics of the competitive response of receptors immobilised to ion-channels which have been incorporated into a tethered bilayer. *Faraday Discuss.* 111:247–258.